Manuscript submitted to AIMS Journal

doi:10.3934/xx.xxxxxxx

STABILITY ANALYSIS OF SOME NEUTRAL DELAY-DIFFERENTIAL EQUATIONS WITH A FREQUENCY-DOMAIN APPROACH

Franco S. Gentile*

Departamento de Matemática, Universidad Nacional del Sur,
Instituto de Investigaciones en Ingeniería Eléctrica (UNS-CONICET),
B8000CPB Bahía Blanca, Argentina

Griselda R. Itovich

Escuela de Producción, Tecnología y Medio Ambiente, Sede Alto Valle y Valle Medio,
Universidad Nacional de Río Negro,
R8336ATG Villa Regina, Argentina

Jorge L. Moiola

Departamento de Ingeniería Eléctrica y Computadoras, Universidad Nacional del Sur,
Instituto de Investigaciones en Ingeniería Eléctrica (UNS-CONICET),
B8000CPB Bahía Blanca, Argentina

(Communicated by the associate editor name)

Abstract. Two general schemes of neutral delay differential equations are considered. They represent non delayed systems with delayed, nonlinear feedback control. The stability conditions in terms of system parameters are derived using an approach based on feedback systems, namely, the Nyquist stability criterion. It is also shown that those results coincide with some already found in the literature, and others derived here, which are based on classical tools, that investigate directly the roots of characteristic equation. Finally, some examples are given to illustrate the usefulness of this approach.

1. **Introduction.** The relevance of delay-differential equations (DDEs) in relation with engineering problems increased enormously in recent years. One of the pioneer textbooks [16] analyzes a wide variety of such equations to solve stability and oscillations problems in mechanics. Most of the contributions concerning DDEs applied to engineering problems, deal with equations of retarded type, which are those that do not present a time-delay in the highest-order derivative of the state variable. Such equations are suitable for modelling a broad diversity of systems in engineering and other areas. For example, an excellent review of the most relevant problems in control systems with time-delay can be seen in [15]. However, in the last few years, the importance of equations of the neutral type increased considerably. Neutral delay-differential equations (NDDEs) are those in which the rate of change of the system at present and past time values depends on present

2020 *Mathematics Subject Classification.* Primary: 34K40, 34K35; Secondary: 93C80.

Key words and phrases. Neutral delay-differential equations, Stability, Frequency-domain method, Nyquist criterion.

This work is supported by grants PGI 24/K087 (UNS) and PI 40/A806 (UNRN).

* Corresponding author: Franco Gentile.

and past values of the states. A precise classification of delay-differential equations can be found in [4]. Several authors arrived to NDDEs when modelling systems in control and mechanical engineering ([20], [21] and [22]) and acoustics ([1], [17]) to mention only a few. In addition, when fast communications are required, the transmission delays are not longer negligible, and also the communication channels are modeled with distributed parameters, then NDDEs may also appear ([5], [10] with implementation on numerical continuation routines in [2], [3]).

The theory of delay-differential equations of retarded type is, by far, much more developed than the corresponding of equations of the neutral type. Even the standard numerical tools for bifurcation analysis, initially focused on retarded equations only [7]. Later, a collocation scheme for numerical investigation of NDDEs was developed in [2] with great success in detecting period-doubled solutions in the route to chaos [3]. By the same time, other techniques seem to be promissory in order to deal with NDDEs [6] and the detection of stability regions. However, as faster applications are required, it is expected that NDDEs will become an important topic in engineering. For this reason, it is essential to develop analysis techniques for NDDEs, which should include their stability and bifurcations.

Graphical tests were used in the past since the pioneering work of Tsypkin [18] enabling the stability analysis for delayed feedback systems in a very original way. That contribution improved necessary criterion to establish oscillations proposed by Barkhausen, which is also still used [1] to delimit the border of instability. More recently, other nearby approaches based on the Cauchy's argument principle were used for DDEs and NDDEs, giving the contributions in [8] and [20]. Following this line, this paper aims to contribute by introducing an analytical technique based on feedback systems, in order to help to understand the dynamical behavior of NDDEs. This technique, namely the frequency-domain approach, was originally developed for ordinary differential equations [11], [12] and then it was extended to DDEs [9]. This approach can be modified to include NDDEs, by simple algebraic manipulations and block algebra of feedback systems. The proposed methodology is used to find the stability regions in the space of system parameters for two general schemes of NDDEs, one of first differential order and another of second order. These results are compared with those found using more classical techniques, namely, those investigating the roots of the characteristic equation. For the first-order model, the stability conditions derived here coincide with those already given in [19].

2. General models of NDDEs.

Two different configurations of neutral delay-differential equations with one delay will be considered. Even if these models are scalar, their stability analysis is not straightforward, as will be seen in short. Moreover, many examples of NDDEs studied in the literature are particular cases of the general structures analyzed below.

2.1. Model of first differential order.

The objective is to study the stability properties of the equilibrium point at $x = 0$, of the following nonlinear equation of the neutral type

$$\dot{x}(t) + \gamma x(t) = \alpha \dot{x}(t-\tau) + \beta x(t-\tau) + h\left(\dot{x}(t-\tau), x(t-\tau)\right), \tag{1}$$

where $\alpha \neq 0$, β and $\gamma > 0$ are real parameters, $\tau > 0$ is the time delay and h is a nonlinear function such that it vanishes simultaneously with its first derivatives at $(0, 0)$. In case that h is a polynomial, it contains quadratic and higher order terms. Notice that in (1), the delay affects the first time-derivative of the state (which is

the highest time-derivative there) and the state itself, thus it is a NDDE. System (1) can be represented in the feedback form

$$\begin{cases} \dot{x}(t) &= Ax(t) + Bg\left(y_1(t), y_2(t)\right), \\ y_1(t) &= y(t-\tau), \quad y_2(t) = \dot{y}(t-\tau), \\ y(t) &= -Cx(t), \end{cases} \tag{2}$$

by choosing the constants $A = -\gamma$, $B = 1$, $C = 1$ and the nonlinear function $g = g(y_1, y_2) = -\alpha y_2 - \beta y_1 + h(-y_2, -y_1)$, where, from (2), one has $(y_1, y_2) = (-x(t-\tau), -\dot{x}(t-\tau))$. The representation (2) is equivalent to a feed-forward plant described by the transfer function $G(s) = C(sI - A)^{-1}B$ plus a delay element given by $e^{-s\tau}$, with a feedback g, as shown in Fig. 1. Notice that s is the complex variable of the Laplace transform. Since the feedback depends on two variables (the delayed output and its derivative), there are two inputs to this block. The plant $G(s)$, together with the delay element and the two-output split can be combined into a single linear block given by

$$G^*(s) = \frac{e^{-s\tau}}{s+\gamma} \begin{bmatrix} 1 \\ s \end{bmatrix}.$$

Thus, the configuration shown in Fig. 1 is equivalent to a single linear plant G^* with a nonlinear feedback given by g.

Clearly, $x = 0$ is an equilibrium point of (1), which translates to $(y_1, y_2) = (0, 0)$ in the feedback representation. According to the frequency-domain approach [11], [12], for the stability analysis, one must consider the Jacobian matrix J of g, computed at the equilibrium, which in this case is simply

$$J = \left[\frac{\partial g}{\partial y_1} \quad \frac{\partial g}{\partial y_2} \right]\Big|_{(y_1,y_2)=(0,0)} = \left[-\beta \quad -\alpha \right]. \tag{3}$$

Then, the Nyquist stability criterion (see [13]) can be applied to the only nonzero eigenvalue of the matrix $G^*(s)J$, namely

$$\lambda(s) = -\frac{(\beta + \alpha s)e^{-s\tau}}{s+\gamma}. \tag{4}$$

In the so called "time-domain", the stability of the equilibrium can be analyzed via the following variational equation, obtained by linearization of (1) around the origin

$$\dot{x}(t) + \gamma x(t) = \alpha \dot{x}(t-\tau) + \beta x(t-\tau), \tag{5}$$

by seeking for solutions of the form $x(t) = ce^{st}$, $c \in \mathbb{R}$, $c \neq 0$, $s \in \mathbb{C}$. Having such a solution of (5) with $s = i\omega$, $\omega \in \mathbb{R}$, translates into the condition $\lambda(i\omega) = -1$ in the "frequency-domain" representation. Moreover, by studying the geometrical locus of $\lambda(i\omega)$ using (4), one can analyze the stability of the equilibrium point.

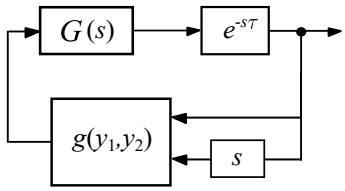

FIGURE 1. Block diagram representing system (1).

Since $\gamma > 0$, the pole of λ at $s = -\gamma$ lies in the left half plane. It means, according to the Nyquist stability criterion [13], that the equilibrium is stable if the locus of $\lambda(i\omega)$ does not enclose the critical point -1 of the complex plane, whereas ω sweeps from 0 to ∞, acting as a free parameter.

For example, since

$$|\lambda(i\omega)| = \frac{|\beta + i\omega\alpha|}{|\gamma + i\omega|} = |\alpha| \frac{|\beta/\alpha + i\omega|}{|\gamma + i\omega|}, \tag{6}$$

it follows that $|\lambda| \to |\alpha|$ when $\omega \to \infty$. Thus, if $|\alpha| > 1$, the geometrical locus encloses the point -1 infinitely many times, asymptotically approaching the circumference $|\lambda| = |\alpha|$. Thus, a necessary stability condition is $|\alpha| < 1$, which will be assumed to hold hereinafter.

On the other hand, from (4), one has $\lambda(0) = -\beta/\gamma$. Thus, in addition to $|\alpha| < 1$, the condition $-\beta/\gamma > -1 \Rightarrow \beta < \gamma$ must hold to ensure stability. On the contrary, if $\beta > \gamma$, the point -1 will be encircled by the Nyquist locus, given that it starts on the negative real axis, at the left of the critical point. Thus, if $\beta > 0$, the equilibrium can loss its stability only via a static bifurcation. This fact is illustrated in Fig. 2.

Since $\gamma > 0$, it is simple to show from (6) that

- If $\gamma > |\beta/\alpha|$, then $|\lambda|$ is monotonously increasing and $|\beta|/\gamma < |\lambda(i\omega)| < |\alpha|$.
- If $\gamma < |\beta/\alpha|$, then $|\lambda|$ is monotonously decreasing and $|\alpha| < |\lambda(i\omega)| < |\beta|/\gamma$.

Both cases are illustrated in Fig. 3. If $\gamma > |\beta/\alpha|$, since $|\lambda| \leq |\alpha| < 1$, the equilibrium is stable (left diagram). On the contrary, if $\gamma < |\beta/\alpha|$, Hopf bifurcations may occur, as can be seen in the right diagram in Fig. 3. Finally, in case that $\gamma = \beta/\alpha$, it results $|\lambda(i\omega)| = |\alpha|$, and the equilibrium is stable if and only if $|\alpha| < 1$. In this case, there is a zero-pole cancellation of $\lambda(s)$, i.e., (4) reduces to $\lambda(s) = -\alpha e^{-s\tau}$. Under $\gamma = \beta/\alpha$, it is possible to define a variable $p(t) := \dot{x}(t) + \gamma x(t)$ and (5) reduces to $p(t) = \alpha p(t - \tau)$, which is a difference equation. Defining also the discrete-time variable $p[n] = p(t)$ for $(n-1)\tau < t < n\tau$, one obtains $p[n] = \alpha p[n-1]$, and the solution of this map is $p[n] = \alpha^n p[0]$. Thus, it follows that the equilibrium $p = 0$ is stable if and only if $|\alpha| < 1$.

From (4), the marginal stability condition $\lambda(i\omega) = -1$ can be written as

$$(\beta + \alpha i\omega)\, e^{-i\omega\tau} = \gamma + i\omega, \tag{7}$$

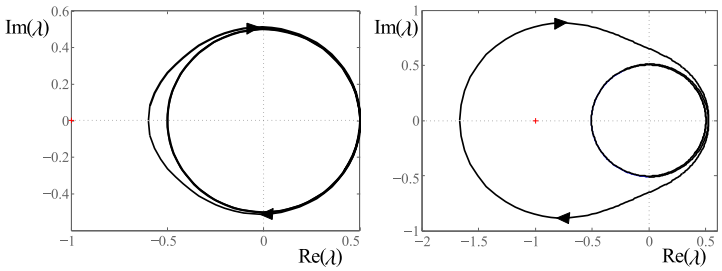

FIGURE 2. Left: Nyquist diagram with $\tau = 1$, $\alpha = 0.5$, $\beta = 0.3$ and $\gamma = 0.5$ ($\lambda(0) = -0.6$, stable equilibrium). Right: Nyquist diagram with $\tau = 1$, $\alpha = 0.5$, $\beta = 0.5$ and $\gamma = 0.3$ ($\lambda(0) \approx -1.66$, unstable equilibrium).

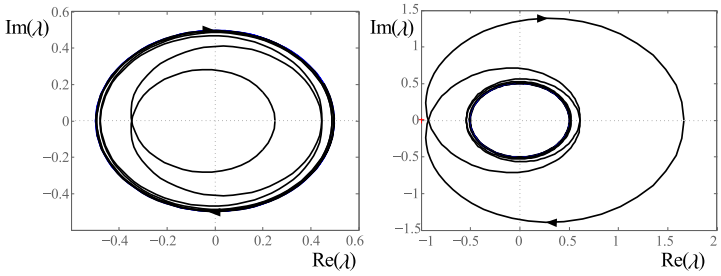

FIGURE 3. Nyquist diagrams for negative values of β. Left: $\tau = 3$, $\alpha = 0.5$, $\beta = -0.2$ and $\gamma = 0.8$ ($\gamma > |\beta|/\alpha = 0.4$). Right: $\tau = 3$, $\alpha = 0.5$, $\beta = -0.5$ and $\gamma = 0.3$ ($\gamma < |\beta|/\alpha = 1$). With $\beta < 0$, it is possible to attain the Hopf bifurcation condition.

which gives $\beta^2 + \alpha^2\omega^2 = \gamma^2 + \omega^2$, and the critical frequency is obtained as

$$\omega_0 = \sqrt{(\beta^2 - \gamma^2)/(1 - \alpha^2)}, \tag{8}$$

which exists if $|\beta| > \gamma$. The condition $\beta = \gamma$ is necessary to produce a static bifurcation, as can be seen letting $\omega = 0$ in (7). Also from (7), it can be obtained

$$-\omega_0\tau = \arctan(\omega_0/\gamma) - \arctan(\alpha\omega_0/\beta), \tag{9}$$

which shows that $\omega_0\tau \in (0, \pi)$. Replacing (8) into (9), and fixing the values of τ and γ, one obtains an implicit relationship that defines the Hopf bifurcation curves in the (α, β) plane. Recall that α and β are control parameters. Thus, by knowing the stability region/s in the (α, β) space, it allows to select appropriate parameter sets in this space, making system (1) stable or unstable. However, (9) is still too complex as to study the shape of those Hopf curves. As an alternative, separating (7) into real and imaginary parts and by applying Cramer's rule under $\omega \neq 0$, it is not difficult to find

$$\beta = \gamma\cos\omega\tau - \omega\sin\omega\tau, \tag{10a}$$

$$\alpha = \cos\omega\tau + \gamma\frac{\sin\omega\tau}{\omega}. \tag{10b}$$

For constant values of γ and τ, (10) allows to plot the Hopf bifurcation curves in the (α, β) plane, using ω as a free parameter, as displayed in Fig. 4 with $\tau = \pi$ and $\gamma = 0.8$. The stability region is shaded in the enlarged diagram. This region is easily identified by direct inspection of the Nyquist diagrams, where no encirclements of the point -1 are observed.

If several values of τ are considered, the corresponding stability regions depicted in Fig. 5 are obtained. In all cases, the upper boundary is given by $\beta = \gamma$, the side boundaries by $|\alpha| = 1$ and the bottom boundary depends on the delay τ, according to (10a). Notice that as long as τ increases, the stability region becomes narrower. In addition, (10) can be interpreted as follows: for each fixed value of α, let ω_0 be the smallest positive solution of (10b). Weedermann [19] showed that there is exactly one solution ω_0 of (10b) in the interval $0 < \omega\tau < \pi$. Thus, the equilibrium is stable if $\gamma\cos\omega_0\tau - \omega_0\sin\omega_0\tau < \beta < \gamma, \quad |\alpha| < 1$. This result agrees with the one given in [19], where it has been proved using a theorem developed by Pontryagin [14].

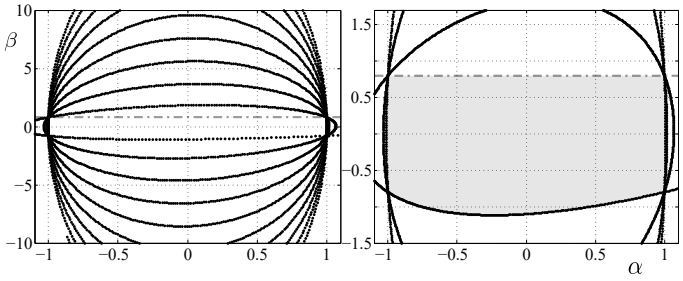

FIGURE 4. Left: Hopf bifurcation curves in the (α, β) plane for system (1) with $\tau = \pi$ and $\gamma = 0.8$. The straight line $\beta = \gamma$ is shown in dashed-dotted line. Right: Enlarged area where the stability region is shaded.

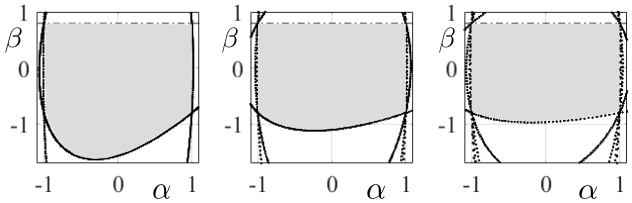

FIGURE 5. Stability regions in the (α, β) plane for $\gamma = 0.8$ and $\tau = \pi/2$ (left), $\tau = \pi$ (center) and $\tau = 3\pi/2$ (right).

2.2. **Model of second differential order.** It is now considered the equation:

$$\ddot{x}(t) + \gamma x(t) = \alpha \ddot{x}(t-\tau) + \beta x(t-\tau) + h(\ddot{x}(t-\tau), x(t-\tau)), \tag{11}$$

where $\alpha \neq 0$, β and $\gamma > 0$ are real parameters, $\tau > 0$ is the time delay and h, again, is a nonlinear function vanishing simultaneously with its first derivatives at $(0,0)$. In order to represent (11) in a feedback form as in the previous case, one may choose $A = -\gamma$, $B = 1$, $C = 1$ and $g = g(y_1, y_2) = -\alpha y_2 - \beta y_1 + h(-y_2, -y_1)$, with $(y_1, y_2) = (-x(t-\tau), -\ddot{x}(t-\tau))$. The block representation is shown in Fig. 6, where $G(s) = 1/(s^2 + \gamma)$, and the output of the block $G(s)$ is $y = -x$. This output is affected by the time-delay, represented by the block $e^{-s\tau}$. Finally, this delayed output splits into two signals, one of them affected by a second-order derivative, exemplified here by s^2. All these operations are linear, thus they can be combined

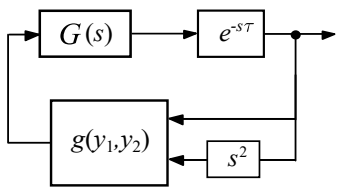

FIGURE 6. Block diagram for system (11).

into a single transfer matrix given by

$$G^*(s) = \frac{e^{-s\tau}}{s^2+\gamma}\begin{bmatrix} 1 \\ s^2 \end{bmatrix}. \tag{12}$$

Since one is interested in the stability properties of the equilibrium point at the origin, the Jacobian matrix for g is the same as in (3), so the unique nonzero eigenvalue of $G^*(s)J$ is

$$\lambda(s) = -\frac{(\beta+\alpha s^2)e^{-s\tau}}{s^2+\gamma}. \tag{13}$$

The critical stability condition established by the Nyquist stability criterion, given by $\lambda(i\omega) = -1$, reads

$$(\beta - \alpha\omega^2)\, e^{-i\omega\tau} = \gamma - \omega^2, \tag{14}$$

or, after separating the real and imaginary parts,

$$\begin{cases} (\beta-\alpha\omega^2)\cos\omega\tau &= \gamma-\omega^2, \\ (\beta-\alpha\omega^2)\sin\omega\tau &= 0. \end{cases} \tag{15}$$

The second equation gives $\omega^2 = \beta/\alpha$ or $\omega = k\pi/\tau$, $k \in \mathbb{Z}$. If $\omega^2 = \beta/\alpha$, it results $\gamma = \beta/\alpha$ after replacing into the first equation. Notice that in this case, there is a zero-pole cancellation in (13), and the characteristic function reduces to

$$\lambda(s)|_{\gamma=\beta/\alpha} = -\alpha e^{-s\tau}, \tag{16}$$

meaning that the geometrical locus lies in a circumference of radius $|\alpha|$. Under this particular combination of parameters, the equilibrium will be stable if $|\alpha| < 1$ and unstable (with infinitely many roots in the right-half plane) if $|\alpha| > 1$. This stability condition under this special situation can also be deduced from the linearized equation of (11) around the equilibrium at $x = 0$, namely

$$\ddot{x}(t) + \gamma x(t) = \alpha\ddot{x}(t-\tau) + \beta x(t-\tau). \tag{17}$$

If $\gamma = \beta/\alpha$, and by defining the variable $p(t) := \ddot{x}(t) + \gamma x(t)$, (17) reduces to $p(t) = \alpha p(t-\tau)$, which is the same map analyzed in the previous case (with a stable fixed point if and only if $|\alpha| < 1$). Hereinafter, it will be considered that $\gamma \neq \beta/\alpha$.

If $\omega = k\pi/\tau$, $k \in \mathbb{Z}$, in (15), it follows that $[\beta - \alpha\,(k\pi/\tau)^2](-1)^k = \gamma - (k\pi/\tau)^2$, giving explicitly the Hopf bifurcation curves in the (α, β) plane for constant values of γ and τ, by replacing $k = 2n+1$ or $k = 2n$, $n \in \mathbb{Z}$, as follows:

- For odd k values: $\beta = (\alpha+1)(2n+1)^2\,(\pi/\tau)^2 - \gamma$.
- For even k values: $\beta = (\alpha-1)(2n)^2\,(\pi/\tau)^2 + \gamma$.

It is necessary to find the stability region (or regions) determined by these straight lines. Since

$$|\lambda(i\omega)| = \frac{|\beta-\alpha\omega^2|}{|\gamma-\omega^2|} = \frac{|\alpha||\omega^2-\beta/\alpha|}{|\omega^2-\gamma|}, \tag{18}$$

thus $|\lambda| \to |\alpha|$ when $\omega \to \infty$, while $\arg(\lambda)$ decreases linearly with the frequency. In other words, for large enough values of ω, the locus of λ will turn around the origin, approaching a circumference of radius $|\alpha|$. If $|\alpha| > 1$, the critical point -1 will be enclosed infinitely many times. Then, a necessary stability condition is $|\alpha| < 1$.

Since the poles of $\lambda(s)$ lie on the imaginary axis, the stability analysis becomes involved, because $|\lambda|$ assumes arbitrarily large values when ω lies in a neighborhood of $\sqrt{\gamma}$. Thus, a modified Nyquist contour must be considered, namely, adding a

half-circumference described by $s = i\sqrt{\gamma} + \epsilon e^{i\theta}$, $-\pi/2 \leq \theta \leq \pi/2$, with $\epsilon \ll 1$, in order to keep the poles outside of the contour. For values of s on this path, $|\lambda(s)|$ will assume large values, and it is necessary to study where this portion of the Nyquist plot (the locus of $\lambda(s)$) will lie, to determine the stability region.

With $s = i\sqrt{\gamma}+\epsilon e^{i\theta}$, $\epsilon \ll 1$, one has $s^2 = -\gamma+i2\sqrt{\gamma}\epsilon e^{i\theta}+\epsilon^2 e^{i2\theta} \simeq -\gamma+i2\sqrt{\gamma}\epsilon e^{i\theta}$, and replacing into (13), it follows that

$$\lambda(s) \simeq -\frac{(\beta - \alpha\gamma + i2\alpha\sqrt{\gamma}\epsilon e^{i\theta})e^{-i\sqrt{\gamma}\tau}e^{-\epsilon\tau e^{i\theta}}}{i2\sqrt{\gamma}\epsilon e^{i\theta}}. \tag{19}$$

The calculations can be simplified by considering $\gamma = 1$ as a first approach, thus the argument or phase of λ becomes

$$\arg(\lambda) = \tfrac{\pi}{2} + \arctan\left(\frac{2\alpha\epsilon\cos\theta}{\beta - \alpha - 2\alpha\epsilon\sin\theta}\right) - \tau - \epsilon\tau\sin\theta - \theta.$$

The second term in the right-hand side not only depends on θ, but also on the relative values of α and β. Let $\psi := \begin{cases} 0, & \beta > \alpha, \\ \pi, & \beta < \alpha, \end{cases}$ then one may compute $\lim_{\epsilon\to 0} \arg(\lambda) = \frac{\pi}{2} - \theta + \psi - \tau$. As long as θ increases, $\arg(\lambda)$ decreases, meaning that the locus of λ rotates in the clockwise sense. As examples, Figs. 7(a)-(b) show the Nyquist diagrams corresponding to $\gamma = 1$, $\tau = \pi/2$, $\alpha = 0.5$, $\beta = 0.8$ and $\gamma = 1$, $\tau = 3\pi/2$, $\alpha = 0.5$, $\beta = 0.8$, respectively. In the diagram in Fig. 7(a), the equilibrium is stable, since the poles of $\lambda(s)$ lie outside of the Nyquist contour and there are no encirclements around the critical point -1. On the contrary, in the case depicted in Fig. 7(b), the equilibrium is unstable, since the locus of λ encloses almost the whole left half plane when $\epsilon \to 0$. The Nyquist diagram has two asymptotes, given by $\arg(\lambda) = \pi + \psi - \tau$ (with $\theta = -\pi/2$) and $\arg(\lambda) = \psi - \tau$ (with $\theta = \pi/2$), following the definition of ψ when $\beta > \alpha$ or $\beta < \alpha$. Observe that with $\gamma = 1$ and $\tau = n\pi$, $n \in \mathbb{N}$, the equilibrium is always unstable since the asymptotes are parallel to the real axis, thus the Nyquist diagram encloses it completely.

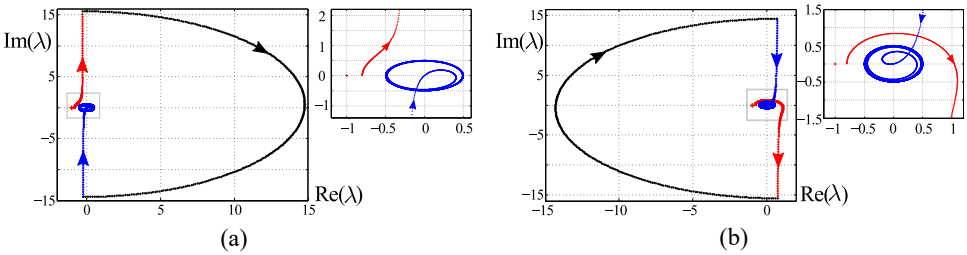

FIGURE 7. (a) Nyquist diagram (and an enlarged area near the origin) with $\gamma = 1$, $\tau = \pi/2$, $\alpha = 0.5$ and $\beta = 0.8$. As $\beta > \alpha$, $\psi = 0$ and the asymptotes are $\arg(\lambda) = \pi - \tau$ and $\arg(\lambda) = -\tau$. For great enough frequencies, the curve lies on the circumference $|\lambda| = |\alpha| = 0.5$. (b) Nyquist diagram (and its corresponding enlargement) with $\gamma = 1$, $\tau = 3\pi/2$, $\alpha = 0.5$ and $\beta = 0.8$. Since $\beta < \alpha$, $\psi = \pi$ and the asymptotes are $\arg(\lambda) = 2\pi - \tau$ and $\arg(\lambda) = \pi - \tau$.

The former calculations can be easily generalized for an arbitrary positive value of γ in (19). In the following analysis, the diagrams shown in Fig. 8 are relevant.

Using (19), one obtains $\lim_{\epsilon\to 0}\arg(\lambda) = \frac{\pi}{2} - \theta + \phi - \sqrt{\gamma}\tau$, where $\phi := \begin{cases} 0, & \beta > \alpha\gamma, \\ \pi, & \beta < \alpha\gamma. \end{cases}$ One needs to consider two cases:

- With $\beta > \alpha\gamma$: One has $\phi = 0$, and $\arg(\lambda)$ decreases from $\pi - \sqrt{\gamma}\tau$ to $-\sqrt{\gamma}\tau$. Observing the right diagram in Fig. 8, a necessary stability condition can be deduced graphically, that is, the plot must not enclose the whole negative real axis. Mathematically, this necessary stability condition can be stated as $-\pi < -\sqrt{\gamma}\tau < 0$. Since $\sqrt{\gamma}\tau$ not necessarily belongs to $(0, \pi)$, this condition can be expressed in a general case as $-(2n+1)\pi < -\sqrt{\gamma}\tau < -2n\pi$, i.e.,
$$2n\pi < \sqrt{\gamma}\tau < (2n+1)\pi, \quad n \in \mathbb{N} \cup \{0\}. \tag{20}$$
The right diagram in Fig. 8 displays a situation in which (20) holds. On the contrary, if $(2n-1)\pi < \sqrt{\gamma}\tau < 2n\pi$, $n \in \mathbb{N}$, the equilibrium is unstable, since the negative real axis is completely enclosed by the Nyquist plot.
- With $\beta < \alpha\gamma$: One has $\phi = \pi$, and $\arg(\lambda)$ decreases from $2\pi - \sqrt{\gamma}\tau$ to $\pi - \sqrt{\gamma}\tau$ (see the center diagram in Fig. 8). This case is analogous, but complementary, of the former one. To prevent the Nyquist plot enclosing completely the negative real axis, the necessary stability condition becomes $-\pi < \pi - \sqrt{\gamma}\tau < 0$, which implies $\pi < \sqrt{\gamma}\tau < 2\pi$. In general form, it can be expressed as
$$(2n-1)\pi < \sqrt{\gamma}\tau < 2n\pi, \quad n \in \mathbb{N}. \tag{21}$$
On the other hand, if $2n\pi < \sqrt{\gamma}\tau < (2n+1)\pi$, $n \in \mathbb{N} \cup \{0\}$, the equilibrium results unstable, since the plot encloses the whole negative real axis, as illustrated in the center diagram in Fig. 8.

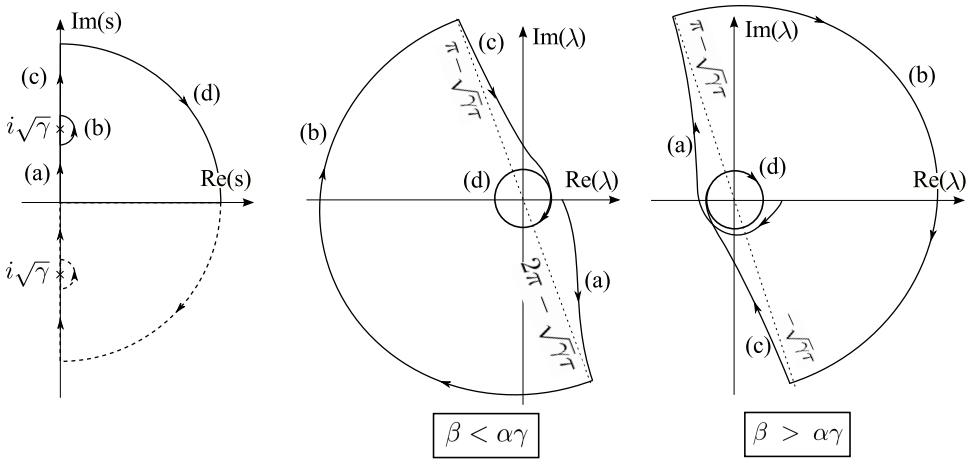

FIGURE 8. The modified Nyquist contour (left) and qualitative representations of the Nyquist diagrams with $\beta < \alpha\gamma$ (center) and $\beta > \alpha\gamma$ (right), for hypothetical values of γ and τ (in this representation, $\sqrt{\gamma}\tau < \pi/2$ holds). The values of $\arg(\lambda)$ determining asymptotes are displayed, since they establish stability conditions. For the hypothetical situations depicted, the necessary stability condition is not fulfilled for $\beta < \alpha\gamma$, but it holds for $\beta > \alpha\gamma$.

The conditions stated in (20) and (21) are necessary in order to have a stable equilibrium point. Additional stability conditions in terms of α and β will be

investigated in the following. In this sense, one needs to analyze the crossings of the Nyquist plot across the real axis. Returning to (13) and letting $\mathrm{Im}(\lambda) = 0$ leads to $\omega^2 = \beta/\alpha$ or $\omega = k\pi/\tau$, $k \in \mathbb{Z}$. But $\omega^2 = \beta/\alpha$ also gives $\mathrm{Re}(\lambda) = 0$, thus this is not a bifurcation condition. Also, since it is enough to consider positive frequencies, only the solutions of the form $\omega_k = k\pi/\tau$, $k \in \mathbb{N}$ are taken into account, and

$$\mathrm{Re}[\lambda(i\omega_k)] = (-1)^{k+1}\frac{[\beta - \alpha(k\pi/\tau)^2]}{\gamma - (k\pi/\tau)^2}, \tag{22}$$

where $\gamma \neq (k\pi/\tau)^2$. In order to simplify calculations, let $\tau = \pi$. Thereby $\omega_k = k$, $k \in \mathbb{N}$, and (22) reduces to

$$\mathrm{Re}[\lambda(i\omega_k)] = (-1)^{k+1}\frac{[\beta - \alpha k^2]}{\gamma - k^2}, \quad \gamma \neq k^2. \tag{23}$$

- With $\beta > \alpha\gamma$: Replacing $\tau = \pi$ into (20), the necessary stability condition reads $2n < \sqrt{\gamma} < 2n + 1$, $n \in \mathbb{N} \cup \{0\}$. Replacing also $k = 0$ into (22), gives $\mathrm{Re}[\lambda(i\omega_0)] = -\beta/\gamma$, and the stability condition is $-\beta/\gamma > -1 \Rightarrow \beta < \gamma$, i.e., $\alpha\gamma < \beta < \gamma$. For $k > 0$, one must analyze to which section of the Nyquist contour belongs each frequency ω_k. For example, for the part (a) shown in Fig. 8, where $0 \leq \omega < \sqrt{\gamma}$, the locus of λ intersects the real axis a finite number of times. Since $\omega < \sqrt{\gamma}$, one has $\beta > \alpha\gamma > \alpha\omega^2 \Rightarrow \beta - \alpha\omega^2 > 0$, thus from (18) it follows that $\partial|\lambda|/\partial\omega = 2\omega(\beta - \alpha\gamma)/(\gamma - \omega^2)^2 > 0$, i.e., $|\lambda|$ is monotonously increasing. It means that the intersection that may cause a stability change is the one produced with greater modulus, corresponding to the highest frequency in that section. Since $2n < \sqrt{\gamma} < 2n+1$ and $k \in \mathbb{N}$, the highest k value for the part (a) is $k = 2n$. For this value, one has $\mathrm{Re}[\lambda(i\omega_{2n})] = -[\beta - \alpha(2n)^2]/[\gamma - (2n)^2]$, and the stability condition $\mathrm{Re}[\lambda(i\omega_{2n})] > -1$ gives

$$\beta < \gamma + (\alpha - 1)(2n)^2. \tag{24}$$

  Graphically, the stability condition above means that the leftmost intersection point of λ with the real axis must lie at the right of the critical point -1.

  With $\omega > \sqrt{\gamma}$, the situation is more complex, since $|\lambda|$ decreases and then increases, as can be seen in the particular example shown in Fig. 9(a) (dark line). However, from (18) it can be deduced that $|\lambda|$ decreases to zero, and then increases, until it approaches asymptotically the value $|\alpha|$. Before reaching the origin, as $|\lambda|$ is decreasing, the intersection with the real axis with greater modulus (the leftmost one) occurs with $\omega = 2n + 1$, the critical frequency immediately higher than $\sqrt{\gamma}$. Replacing $k = 2n + 1$ into (23), the stability condition $\mathrm{Re}[\lambda(i\omega_{2n+1})] > -1$ results in

$$\beta < -\gamma + (\alpha + 1)(2n + 1)^2. \tag{25}$$

  Figure 9(b) displays the stability region obtained with $\gamma = (4.5)^2$ and $\tau = \pi$. Its boundaries are given by (24)-(25) with $n = 2$ ($4 < \sqrt{\gamma} < 5$), and $\beta = \alpha\gamma$.

- With $\beta < \alpha\gamma$: The necessary stability condition, assuming $\tau = \pi$ in (21), is $2n-1 < \sqrt{\gamma} < 2n$, $n \in \mathbb{N}$. Again, if $k = 0$ in (22), the stability condition reads $\mathrm{Re}[\lambda(i\omega_0)] = -\beta/\gamma > -1 \Rightarrow \beta < \gamma$, which holds since $\beta < \alpha\gamma$ and $\alpha < 1$. With $0 \leq \omega < \sqrt{\gamma}$, once again λ intersects the real axis a finite number of times. However, $|\lambda|$ is not monotonously increasing or decreasing, as can be deduced easily from (18). For example, Fig. 10(a) shows a detail of the Nyquist diagram with $\gamma = (3.5)^2$, $\tau = \pi$, $\alpha = 0.5$ and $\beta = 4$, where the light line corresponds to $0 \leq \omega < \sqrt{\gamma}$. From (18), it follows that $|\lambda|$ is decreasing

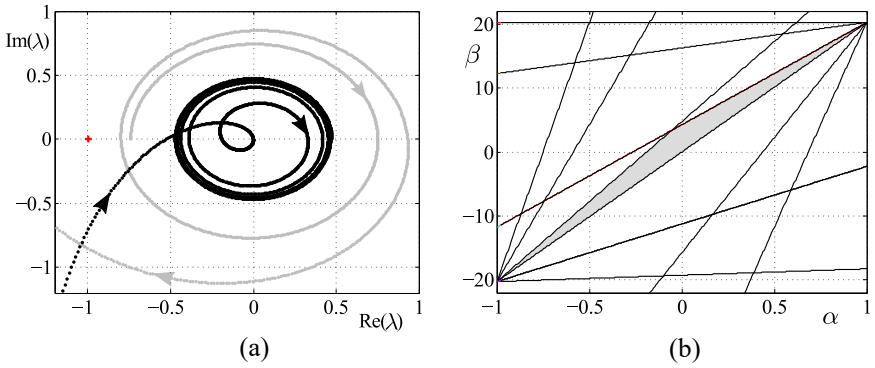

FIGURE 9. (a) Detail of the Nyquist diagram obtained with $\gamma = (4.5)^2$, $\tau = \pi$, $\alpha = 0.5$ and $\beta = 15$. Light line corresponds to $\omega < \sqrt{\gamma}$ and dark line corresponds to $\omega > \sqrt{\gamma}$. (b) Stability region with $\gamma = (4.5)^2$ and $\tau = \pi$.

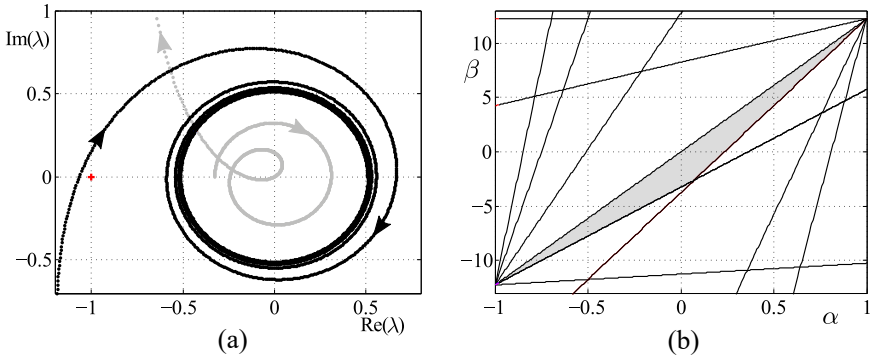

FIGURE 10. (a) Detail of the Nyquist diagram with $\gamma = (3.5)^2$, $\tau = \pi$, $\alpha = 0.5$ and $\beta = 4$. Light line corresponds to $\omega < \sqrt{\gamma}$ and dark line corresponds to $\omega > \sqrt{\gamma}$. (b) Stability region with $\gamma = (3.5)^2$ and $\tau = \pi$.

for $0 < \omega < \sqrt{|\beta/\alpha|}$ and increasing for $\omega > \sqrt{|\beta/\alpha|}$. With $0 < \omega < \sqrt{|\beta/\alpha|}$ it holds that $|\lambda| < |\beta|/\gamma = |\lambda(0)|$, so if $|\beta| < \gamma$, no encirclement of -1 can be introduced for these ω values. With $\omega > \sqrt{|\beta/\alpha|}$, as $|\lambda|$ is increasing, the intersection that may cause a stability change is the one observed with greater modulus, corresponding to the highest critical frequency in that portion. Since $2n-1 < \sqrt{\gamma} < 2n$, $k \in \mathbb{N}$, that frequency for the part (a) of the corresponding diagram in Fig. 8 is $k = 2n-1$. For this value, one has $\mathrm{Re}[\lambda(i\omega_{2n-1})] = [\beta - \alpha(2n-1)^2]/[\gamma - (2n-1)^2]$, and the stability condition $\mathrm{Re}[\lambda(i\omega_{2n-1})] > -1$ becomes

$$\beta > -\gamma + (\alpha+1)(2n-1)^2. \tag{26}$$

When $\omega > \sqrt{\gamma}$, the situation is much simpler, and from (18) it is easy to show that $|\lambda|$ is monotonously decreasing verifying that $\partial|\lambda|/\partial\omega < 0$. It means that the intersection between the Nyquist diagram and the real axis causing a stability change, occurs for the critical frequency immediately greater than

$\sqrt{\gamma}$, i.e., $\omega = 2n$. Replacing $k = 2n$ into (23), the stability condition given by $\mathrm{Re}[\lambda(i\omega_{2n})] > -1$ becomes

$$\beta > \gamma + (\alpha - 1)(2n)^2. \tag{27}$$

The stability region is displayed in Fig. 10(b) for $\gamma = (3.5)^2$ and $\tau = \pi$. Its boundaries are given by (26)-(27) with $n = 2$ ($3 < \sqrt{\gamma} < 4$) and $\beta = \alpha\gamma$.

The previous results can be generalized for an arbitrary value of τ, using (22) instead of (23). Reproducing the calculations above leads to the following result.

Theorem 2.1. *Consider system (11) and assume $|\alpha| < 1$, $\beta \neq \gamma\alpha$. The equilibrium point at $x = 0$ is stable if and only if the following inequalities are satisfied:*

- *With $\beta > \alpha\gamma$: $\beta < \gamma+(\alpha-1)(2n)^2(\pi/\tau)^2$ and $\beta < -\gamma+(\alpha+1)(2n+1)^2(\pi/\tau)^2$, where $n \in \mathbb{N} \cup \{0\}$ is such that $2n\pi < \sqrt{\gamma}\tau < (2n+1)\pi$.*
- *With $\beta < \alpha\gamma$: $\beta > -\gamma+(\alpha+1)(2n-1)^2(\pi/\tau)^2$ and $\beta > \gamma+(\alpha-1)(2n)^2(\pi/\tau)^2$, where $n \in \mathbb{N}$ is such that $(2n-1)\pi < \sqrt{\gamma}\tau < 2n\pi$.*

The above results can be also obtained by an independent approach, namely, using a classical technique that studies the location of the roots of the characteristic equation of (17). By substituting a trial solution $x(t) = ce^{st}$, with $c \neq 0$, $s \in \mathbb{C}$ into (17), and multiplying by $e^{s\tau}$, gives

$$P(s) = e^{s\tau}(s^2 + \gamma) - \alpha s^2 - \beta = 0. \tag{28}$$

Recall that $\alpha \neq 0$, β and $\gamma, \tau > 0$ are real parameters, and notice that $P(s)$ is an exponential polynomial with a principal term given by $e^{s\tau}s^2$. Let $P(iy) = F(y)+iG(y)$, $y \in \mathbb{R}$. The following results [4], [14] can be applied for the alternative stability analysis.

Theorem 2.2 (Pontryagin)**.** *If all the zeros of P are located on the left half plane, then all the zeros of F and G are real, alternating and $F(y)G'(y) - F'(y)G(y) > 0$, for all $y \in \mathbb{R}$.*

Theorem 2.3 (Pontryagin)**.** *All the zeros of P are located on the left half plane if I) all the roots of F are real and for each of these zeros the condition $F'(y)G(y) < 0$ is satisfied, or, II) all the roots of G are real and for each of these zeros the condition $F(y)G'(y) > 0$ is satisfied, or, III) all the roots of F and G are real and alternate and the inequality $F(y)G'(y) - F'(y)G(y) > 0$ is valid for at least one value of y.*

Substituting $s = i\omega$ into (28), making the variable change $z = \omega\tau$, and separating into real and imaginary parts, yields

$$F(z) = \cos z\ (\gamma\tau^2 - z^2) + \alpha z^2 - \beta\tau^2 = 0, \qquad G(z) = \sin z\ (\gamma\tau^2 - z^2) = 0. \tag{29}$$

The roots of $G(z)$ are $z_k = k\pi, k \in \mathbb{Z}$, and $\bar{z}_{1,2} = \pm\tau\sqrt{\gamma}$. In order to simplify the following exposition, consider $\tau = \pi$. As $\gamma > 0$, all the roots of G are real as is required in Theorem 2.3 II). Moreover, it is not difficult to show that (28) has at least one solution with positive real part if $|\alpha| > 1$. Thus, the assumption $|\alpha| < 1$ is made hereinafter. To prevent F and G having common roots, neither of the following equations must be satisfied

$$\beta = [(-1)^{k+1} + \alpha]k^2 + \gamma(-1)^k, \qquad \alpha\gamma - \beta = 0. \tag{30}$$

Also, it is simple to verify that the roots of G are simple if $\gamma \neq k^2$.

The condition II) in Theorem 2.3 will be used to give sufficient stability conditions for system (11). It is required that $F(z)G'(z) > 0$ for any root z of G. One can divide the analysis in the following cases: **(1)** $0 < \gamma < 1$, and **(2)** $k^2 < \gamma < (k+1)^2$, the latter with two sub-cases: **(2A)** k even or **(2B)** k odd. Since FG' is an even function, it is enough to consider only positive values of k and the root $\bar{z}_1$ of G.

(1) Let $0 < \gamma < 1$. From (29), it follows that $F(0)G'(0) > 0$ implies $\beta < \gamma$. Besides $F(\bar{z}_1) = (\alpha\gamma - \beta)\pi^2$ and $G'(\bar{z}_1) = \sin\bar{z}_1(-2\bar{z}_1) < 0$ (since $0 < \bar{z}_1 < \pi$). Thus $F(\bar{z}_1)G'(\bar{z}_1) > 0$ implies $\alpha\gamma < \beta$. For the roots $z_k = k\pi$ of G with k even, one has

$$F(k\pi) = \pi^2[k^2(\alpha - 1) + \gamma - \beta], \quad G'(k\pi) = \pi^2(\gamma - k^2), \tag{31}$$

and to verify $F(k\pi)G'(k\pi) > 0$ it must be certain that $k^2(\alpha - 1) + \gamma - \beta < 0$, i.e., $\beta > k^2(\alpha - 1) + \gamma$. But this condition is already fulfilled if $\alpha\gamma < \beta$, the inequality obtained with $\bar{z}_1$, since $\alpha < 1$. On the other hand, for $z_k = k\pi$ with k odd, one has

$$F(k\pi) = \pi^2[k^2(\alpha + 1) - \gamma - \beta], \quad G'(k\pi) = \pi^2(k^2 - \gamma), \tag{32}$$

and the condition $F(k\pi)G'(k\pi) > 0$ gives $\beta < k^2(\alpha + 1) - \gamma$, where k is an odd, positive integer. Under the assumption $-1 < \alpha < 1$, all of them are satisfied if the one corresponding to $k = 1$ holds, i.e., if $\beta < \alpha + 1 - \gamma$.

Thus, one can summarize the stability conditions with $0 < \gamma < 1$, as follows:

$$|\alpha| < 1, \quad \beta < \gamma, \quad \gamma\alpha < \beta < \alpha + 1 - \gamma.$$

(2) Consider $1 < k^2 < \gamma < (k + 1)^2$.
(2A) With k even. The condition $F(0)G'(0) > 0$ gives again $\beta < \gamma$. For the root $\bar{z}_1 \in (k\pi, (k + 1)\pi)$, one has $F(\bar{z}_1) = (\alpha\gamma - \beta)\pi^2$ and $G'(\bar{z}_1) = \sin\bar{z}_1(-2\bar{z}_1) < 0$, thereby $F(\bar{z}_1)G'(\bar{z}_1) > 0$ implies $\alpha\gamma < \beta$.

Using (31) with $\gamma > k^2$, the condition $F(k\pi)G'(k\pi) > 0$ leads to $\beta < k^2(\alpha-1)+\gamma$. By replacing the root $z_{k+1} = (k + 1)\pi$ into F and G', it is simple to verify that the condition $F(z_{k+1})G'(z_{k+1}) > 0$ implies $\beta < (k + 1)^2(\alpha + 1) - \gamma$.

It is also necessary to analyze the cases where $z = j\pi$, with $j < k$ or $j > k + 1$.

- Consider $j < k$, with j even. One can replace k by j into (31) to find that $F(j\pi)G'(j\pi) > 0$ holds if $j^2(\alpha - 1) + \gamma - \beta > 0$, but this is always certain if $\beta < k^2(\alpha - 1) + \gamma$, since $\alpha < 1$.
- Consider $j < k$, with j odd. Replacing k by j into (32), the condition $F(j\pi)G'(j\pi) > 0$ gives $j^2(\alpha+1)-\gamma-\beta < 0$, but this is verified provided that $\beta > \alpha\gamma > j^2(\alpha + 1) - \gamma$, due to $-1 < \alpha$.
- Consider $j > k + 1$, with j even. Using (31), the condition $F(j\pi)G'(j\pi) > 0$ holds if $j^2(\alpha-1)+\gamma-\beta < 0$, which is satisfied as long as $\beta > \alpha\gamma > j^2(\alpha-1)+\gamma$, given that $\alpha < 1$.
- Consider $j > k + 1$, with j odd. From (32), the condition $F(j\pi)G'(j\pi) > 0$ gives $j^2(\alpha+1)-\gamma-\beta > 0$, which holds immediately if $\beta < (k+1)^2(\alpha+1)-\gamma$ with $-1 < \alpha$.

One can summarize the stability conditions with $k^2 < \gamma < (k + 1)^2$, k even, as:

$$|\alpha| < 1, \quad \alpha\gamma < \beta < \gamma, \quad \beta < k^2(\alpha - 1) + \gamma, \quad \text{and} \quad \beta < (k + 1)^2(\alpha + 1) - \gamma.$$

(2B) With k odd. The condition $F(0)G'(0) > 0$ leads again to $\gamma > \beta$. For the root $\bar{z}_1 \in (k\pi, (k+1)\pi)$, it follows that $F(\bar{z}_1) = (\alpha\gamma-\beta)\tau^2$ and $G'(\bar{z}_1) = \sin\bar{z}_1(-2\bar{z}_1) > 0$, so the condition $F(\bar{z}_1)G'(\bar{z}_1) > 0$ leads to $\beta < \alpha\gamma$. As k is odd, using (32) one can

verify that $F(k\pi)G'(k\pi) > 0$ yields $\beta > k^2(\alpha+1) - \gamma$. On the other hand, as $F(z_{k+1}) = \pi^2(k+1)^2\left[(\alpha-1)+\gamma\right] - \beta\pi^2$ and $G'(z_{k+1}) = \pi^2[-(k+1)^2+\gamma] < 0$, the condition $F(z_{k+1})G'(z_{k+1}) > 0$ gives $\beta > (k+1)^2(\alpha-1)+\gamma$.

It is again necessary to analyze the cases where $z = j\pi$, with $j < k$ or $j > k+1$, where j may be even or odd. One may proceed analogously as in case **(2A)**. The details are omitted here for short. Thus, the summary of stability conditions with $k^2 < \gamma < (k+1)^2$, k odd, is:

$$|\alpha| < 1, \quad \beta < \alpha\gamma, \quad \beta > k^2(\alpha+1) - \gamma, \quad \text{and} \quad \beta > (k+1)^2(\alpha-1)+\gamma.$$

The former analysis gives sufficient conditions for P (see (28)) to have all its roots with negative real part. Those conditions are also necessary for the stability, as it is proved in the Appendix. Thus, the main result is stated as follows.

Theorem 2.4. *Consider (28) with $\alpha \neq 0, \beta \in \mathbb{R}$, $\gamma, \tau > 0$. It is assumed that neither of the equations in (30) is satisfied. Suppose $\tau = \pi$ and $\gamma \neq k^2$, $k \in \mathbb{Z}$. All the roots of P (28) lie on the left-half plane if and only if, the following inequalities are verified, while $|\alpha| < 1$ and $\beta < \gamma$:*

(1) *If $0 < \gamma < 1$, then $\gamma\alpha < \beta < \alpha + 1 - \gamma$.*
(2) *If $k^2 < \gamma < (k+1)^2$, $k \in \mathbb{N}$,*
(2A) *If k is even, then $\alpha\gamma < \beta$, $\beta < k^2(\alpha-1)+\gamma$ and $\beta < (k+1)^2(\alpha+1)-\gamma$.*
(2B) *If k is odd, then $\beta < \alpha\gamma$, $\beta > k^2(\alpha+1)-\gamma$ and $\beta > (k+1)^2(\alpha-1)+\gamma$.*

Notice that even if Theorems 2.1 and 2.4 are stated in slightly different ways (replace $\tau = \pi$ in the former theorem), they are completely equivalent.

3. Examples.

In this section, a couple of examples of nonlinear systems will be considered. For their stability analysis, the linearized equations studied in Section 2 are relevant.

3.1. Chua's circuit with lossless transmission line.

Consider the Chua's circuit consisting of a resistor R, a capacitor C_1 and a nonlinear diode D, connected to a long lossless transmission line. This realization, proposed in [10], is shown schematically in Fig. 11. The model is developed as a system of partial differential equations, since it has distributed parameters. Nevertheless, by using the D'Alembert's wave equation, it can be reduced into a single NDDE, which according to [10], is given by

$$C_1\left[\dot{x}(t) - q\dot{x}(t-\tau)\right] = \tfrac{-1}{Z+R}\left[x(t) + x(t-\tau)\right] - g\left(x(t) - qx(t-\tau) - E\right), \qquad (33)$$

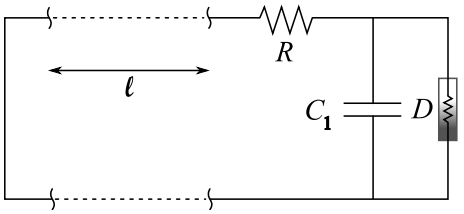

FIGURE 11. Realization of the Chua's circuit connected to a long lossless transmission line of length ℓ. The nonlinear element known as Chua's diode is labeled as D.

with $Z = \sqrt{L/C}$, where L and C are the inductance and capacity, respectively, of the transmission line (per unit length), and $q = (Z-R)/(Z+R)$. There is an offset voltage E in the nonlinear element, which is assumed to be zero. The delay of the transmission line is denoted by τ, and $g(x) = ax+bx^3$ is the nonlinear characteristic of the Chua's diode. The state variable x represents a scaled version of the voltage across D. Liao [10] analyzed the stability and bifurcations of the equilibrium point at $x = 0$. If a small perturbation around $x = 0$ is considered in (33), the linearized equation, after regrouping terms, results

$$\dot{x}(t) + \tfrac{1}{C_1}\left(\tfrac{1}{Z+R} + a\right)x(t) = q\dot{x}(t-\tau) + \tfrac{1}{C_1}\left(aq - \tfrac{1}{Z+R}\right)x(t-\tau).$$

It is simple to verify that equation above is in the form (5), with

$$\gamma = \tfrac{1}{C_1}\left(\tfrac{1}{Z+R} + a\right), \quad \alpha = q, \quad \beta = \tfrac{1}{C_1}\left(aq - \tfrac{1}{Z+R}\right). \tag{34}$$

For system (1), the stability conditions were expressed in terms of parameters α and β, since they represent control parameters. In Chua's circuit, the usual control parameters are R and a (they can be handled by using variable resistances). Thus, it would be convenient to express the stability conditions in terms of R and a. By replacing $q = (Z-R)/(Z+R)$ into (34), it is not difficult to find that

$$R = Z(1-\alpha)/(1+\alpha), \qquad a = \frac{1+\alpha}{2\alpha Z} + \frac{\beta}{\alpha}C_1. \tag{35}$$

Using (35), and from the knowledge of the stability region for system (1), one can choose values of α and β corresponding to a stable (unstable) equilibrium, and then compute the corresponding values of R and a from (35) to produce a stable (unstable) equilibrium in system (33).

As particular examples, in [10] the author performed numerical simulations of (33) with $Z = 25$, $R = 5$, $C_1 = 0.1$, $\tau = 1$ and $a = 0.05$ (he found a stable equilibrium) and with $Z = 25$, $R = 5$, $C_1 = 0.1$, $\tau = 1$ and $-a = 0.05$ (he found an unstable equilibrium). The Nyquist diagrams corresponding to those parameter sets are shown in Fig. 12. The results here agree with those reported in [10].

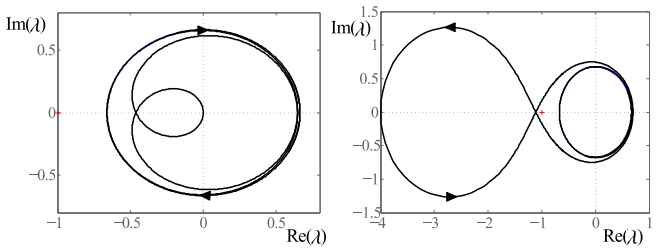

FIGURE 12. Left: Nyquist diagram for system (33) with $Z = 25$, $R = 5$, $C_1 = 0.1$, $\tau = 1$ and $a = 0.05$ (the equilibrium is stable). Right: Nyquist diagram with $Z = 25$, $R = 5$, $C_1 = 0.1$, $\tau = 1$ and $-a = 0.05$ (the equilibrium is unstable).

3.2. **Mechanical system with delayed force control.** Another interesting example, is the mechanical system with force control presented in [22], which is shown schematically in Fig. 13. There is a mass m coupled to a fixed frame through a spring of stiffness k_1. Another spring of stiffness k_2 ($k_2 \gg k_1$) is a sensor, measuring

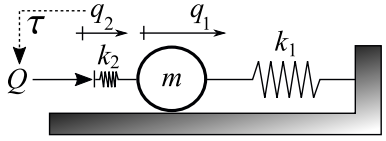

FIGURE 13. Mechanical system with force control studied in [22].

the displacement q_2, which is sent to the controller. It is assumed that the control is affected by a time delay τ. This scenario may occur, for example, in robotic teleoperation, where the transmission delay cannot be neglected. It is considered a proportional control, of gain P. The basic expression of the control action is $Q = -P(F_m - F_d) + F_m$, $F_m = k_2 q_2$, where F_m and F_d are the measured and desired forces, respectively. However, by including the saturation effect of the control action and the time-delay, the following expression is more accurate

$$Q = -F_s \tanh\left(\tfrac{P}{F_s}\left[k_2 q_2(t-\tau) - F_d\right]\right) + k_2 q_2(t-\tau).$$

After writing the equations of movement based on Newton's laws, replacing the expression of the control action, and by scaling both the time and the state variables, the authors in [22] finally arrive to the model

$$\begin{aligned} \ddot{x}(t) + (\omega_n\tau)^2 x(t) =& \ddot{x}(t-1) + (\omega_n\tau)^2 x(t-1) \\ & - (\omega_n\tau)^2 \tanh\left(P\left[\tfrac{1}{(\omega_n\tau)^2}\ddot{x}(t-1) + x(t-1)\right]\right), \end{aligned} \tag{36}$$

where $\omega_n \approx \sqrt{k_1/m}$ is the natural oscillation frequency of the uncontrolled system. The linearized equation around the equilibrium in $x = 0$ can be arranged as

$$\ddot{x}(t) + (\omega_n\tau)^2 x(t) = (1-P)\ddot{x}(t-1) + (\omega_n\tau)^2(1-P)x(t-1).$$

Equation above has the structure of (17), with $\gamma = (\omega_n\tau)^2$, $\alpha = 1 - P$ and $\beta = \gamma(1-P)$. Thus, the condition $\gamma = \beta/\alpha$ is verified. It gives the particular situation given by (16). Recall that, under this condition, the equilibrium is stable if $|\alpha| < 1$ and infinitely unstable if $|\alpha| > 1$. Then, the system is stable if $|1 - P| < 1 \iff 0 < P < 2$, and it does not depend on the delay. This result coincides with the conclusion arrived in [22] but using a different approach.

4. **Conclusions.** The analysis of NDDEs is a challenging field and here the frequency domain approach has been used in order to extend the results from the corresponding study of equations of retarded type in [9]. A simple block manipulation allows to consider certain NDDEs, in order to study their stability and bifurcations so results are very auspicious to extend the technique to analyze more complicated models.

The counterpart analysis via "time-domain" techniques may become very sophisticated, specially if the roots of the real and imaginary parts of the characteristic equation cannot be explicitly computed, as can be seen in [19]. Even if those roots can be computed, the stability analysis may be very involved, as can be appreciated from the proof of Theorem 2.4.

Thus, the graphical interpretation provided by the Nyquist criterion simplifies the stability analysis by a great extent. Though the frequency-domain method is introduced here for scalar NDDEs, it is straightforward to extend it to multivariable input-multivariable output systems due to application of the generalized Nyquist

stability criterion [11]. The key point here is to compute the so-called characteristic gain loci which are like different transfer functions, sweeping on the Nyquist contour, and see if they enclose the critical point -1. These characteristic gain loci belong to an algebraic function defined on an appropriate Riemann surface. In simple words, this is a trade-off when modelling systems between input-output box (external model) and the state-space approach (internal model). Moreover, the amplitude and frequency of the emerging periodic solution via Hopf bifurcation can be obtained from the current approach but this will be communicated elsewhere.

Acknowledgments. The financial support of grants PGI 24/K087 (Universidad Nacional del Sur) and PI 40/A806 (Universidad Nacional de Río Negro) is greatly appreciated.

REFERENCES

[1] R. Auvray, B. Fabre and P. -Y. Lagrée, Regime change and oscillation thresholds in recorder-like instruments, *J. Acoust. Soc. Am.*, **131**(2) (2012), 1574–1585.
[2] D. A. W. Barton, B. Krauskopf and R. E. Wilson, Collocation schemes for periodic solutions of neutral delay differential equations, *J. of Diff. Eqns. and Apps.*, **12**(11) (2006), 1087–1101.
[3] D. A. W. Barton, B. Krauskopf and R. E. Wilson, Bifurcation analysis tools for neutral delay equations: A case study, *IFAC Proceedings Volumes*, **39**(10) (2006), 36–41.
[4] R. Bellman and K. Cooke, *Differential Difference Equations*, Academic Press, New York, 1963.
[5] J. N. Blakely and N. J. Corron, Experimental observation of delay-induced radio frequency chaos in a transmission line oscillator, *Chaos*, **14**(4) (2004), 1035–1041.
[6] D. Breda, S. Maset and R. Vermiglio, Pseudospectral approximation of eigenvalues of derivative operators with non-local boundary conditions, *Applied Num. Math.*, **56**(3/4) (2006), 318–331.
[7] K. Engelborghs, T. Luzyanina and D. Roose, Numerical bifurcation analysis of delay differential equations using DDE-BIFTOOL, *ACM Trans. on Math. Soft.*, **28**(1) (2002), 1–21.
[8] M. Fu, A. W. Olbrot and M. P. Polis, Robust stability for time-delay systems: The edge theorem and graphical tests, *IEEE Trans. on Autom. Contr.*, **34** (1989), 813–820.
[9] F. Gentile, J. L. Moiola and G. Chen, *Frequency-domain Approach to Hopf Bifurcation Analysis: Continuous Time-delayed Systems*, World Scientific Publishing Co, Singapore, 2019.
[10] X. Liao, Dynamical behavior of Chua's circuit with lossless transmission line, *IEEE Trans. Circ. Syst. I*, **63**(2) (2016), 245–255.
[11] A. I. Mees, *Dynamics of Feedback Systems*, John Wiley and Sons, Chichester, UK, 1981.
[12] J. L. Moiola and G. Chen, *Hopf Bifurcation Analysis: A Frequency Domain Approach*, World Scientific Publishing Co, Singapore, 1996.
[13] K. Ogata, *Modern Control Engineering*, Prentice Hall, Boston, 2010.
[14] L. S. Pontryagin, On the zeros of some elementary transcendental functions, *Amer. Math. Soc. Transl.* **2**(1) (1955), 95–110.
[15] R. Sipahi, S. I. Niculescu, C. T. Abdallah, W. Michiels and K. Gu, Stability and stabilization of systems with time delay, *IEEE Control Syst. Mag.*, **31** (2011), 38–65.
[16] G. Stépán, *Retarded Dynamical Systems: Stability and Characteristic Functions*, Pitman Research Notes in Math. Series 210, Longman Scientific and Technical, 1989.
[17] S. Terrien, R. Auvray, B. Fabre, P. -Y. Lagrée and C. Vergez, Numerical resolution of a physical model of flute-like instruments: Comparison between different approaches, *Acoustics 2012, Proceedings of the Acoustics*, (2012), 1179–1184.
[18] Y. Z. Tsypkin, Stability of systems with delayed feedback, *Automat. Telemekh.*, **7** (1946), 107–129. (reprinted in Frequency Response Methods in Control Systems, MacFarlane A. G. J. (Editor), IEEE Press, 45–56, 1979).
[19] M. Weedermann, Hopf bifurcation calculations for scalar neutral delay differential equations, *Nonlinearity*, **19**(9) (2006), 2091–2102.
[20] Q. Xu, and Z. H. Wang, Exact stability test of neutral delay differential equations via rough estimation of the testing integral, *Int. J. Dynam. Control*, **2** (2014), 154–163.

[21] L. Zhang, G. Stépán and T. Insperger, Saturation limits the contribution of acceleration feedback to balancing against reaction delay, *J. R. Soc. Interface*, **15** (2018), http://dx.doi.org/10.1098/rsif.2017.0771.
[22] L. Zhang and G. Stépán, Bifurcations in basic models of delayed force control, *Nonlinear Dynamics*, **99** (2020), 99–108.

Appendix

It will be shown that the hypotheses in Theorem 2.4 are also necessary for the stability of the equilibrium point of system (11). It is supposed that all the roots of P (28) lie in the left-half plane. Thus Theorem 2.2 guarantees that all the zeros of F and G (see 29) are real and alternating. Using a related result [4], if $\gamma > 0$, $\tau = \pi$ and $\gamma \neq k^2$, it can be deduced G has $4n+2$ roots in any interval of the form $[-2n\pi + \pi/2, 2n\pi + \pi/2]$, supposing that $\gamma \in \left((n-1)^2, n^2\right)$ for certain $n \in \mathbb{N}$. The roots of G are $z_k = k\pi, k \in \mathbb{Z}$ and $\bar{z}_{1,2} = \pm\sqrt{\gamma}\pi$. Since

$$F(0) = (\gamma - \beta)\pi^2, \quad F(\sqrt{\gamma}\pi) = (\alpha\gamma - \beta)\pi^2, \tag{A1}$$

the conditions $F(0) \neq 0$ and $F(\pm\sqrt{\gamma}\pi) \neq 0$ give $\gamma \neq \beta$ and $\alpha\gamma \neq \beta$, respectively. Moreover, from (29) the roots z of F satisfy $\cos z = \alpha - (\alpha\gamma - \beta)\pi^2/(\gamma\pi^2 - z^2)$ and they must be countable and infinite. Since $\lim_{z\to\infty} (\alpha\gamma - \beta)\pi^2/(\gamma\pi^2 - z^2) = 0$, if $|\alpha| \geq 1$ there is possibly only a finite set of roots of F in $\mathbb{R}$. Thus, in all the reasoning that follows, it is assumed that the condition $|\alpha| < 1$ holds. The analysis is divided again according to the values of γ. Suppose that:

(1) $0 < \gamma < 1$. Consider the roots of G given by $0, \sqrt{\gamma}\pi$ and π. From (A1), one has $\gamma \neq \beta$ and $\alpha\gamma \neq \beta$. Taking into account the alternation of the roots of F and G, if $\beta < \gamma$, then $F(0) > 0$. Also if $\alpha\gamma - \beta < 0$ then $F(\sqrt{\gamma}\pi) < 0$, and finally if $F(\pi) > 0$, it follows that $\beta < \alpha + 1 - \gamma$. On the contrary, if $\gamma < \beta$ results $F(0) < 0$, but if $\alpha\gamma - \beta < 0$, $F(\sqrt{\gamma}\pi) < 0$, and the roots of F do not necessarily alternate. But if $F(\sqrt{\gamma}\pi) > 0$, it follows $\alpha\gamma - \beta > 0$ which is an absurd since $\gamma < \beta$ and $\alpha < 1$. Thereby, one concludes that $\beta < \gamma$. So if $0 < \gamma < 1$, one needs $\alpha\gamma < \beta < \gamma$ and $\beta < \alpha + 1 - \gamma$.

(2) Suppose now $k^2 < \gamma < (k+1)^2$, $k > 1$, and consider the roots $k\pi$, $\sqrt{\gamma}\pi$ and $(k+1)\pi$ of G.

(2A) Let k be even, then

$$\begin{gathered} F(k\pi) = [k^2(\alpha - 1) + \gamma - \beta]\pi^2, \qquad F(\sqrt{\gamma}\pi) = (\alpha\gamma - \beta)\pi^2, \\ F((k+1)\pi) = [(k+1)^2(\alpha + 1) - \gamma - \beta)]\pi^2. \end{gathered} \tag{A2}$$

Provided that the roots of G alternate with those of F, it follows that if $\alpha\gamma - \beta < 0$, from (A2) results $F(\sqrt{\gamma}\pi) < 0$ and it should be $F(k\pi) > 0$ and $F((k+1)\pi) > 0$, giving $\beta < k^2(\alpha - 1) + \gamma$ and $\beta < (k+1)^2(\alpha + 1) - \gamma$. On the other hand, if $\alpha\gamma - \beta > 0$, using (A2) again, results $F(\sqrt{\gamma}\pi) > 0$ and it should be $F(k\pi) < 0$ and $F((k+1)\pi) < 0$, giving $\beta > k^2(\alpha - 1) + \gamma$ and $\beta > (k+1)^2(\alpha + 1) - \gamma$. However, as $|\alpha| < 1$, the condition $\alpha\gamma > \beta > k^2(\alpha - 1) + \gamma$ implies $\gamma < k^2$ which is an absurd. Besides $\alpha\gamma > \beta > (k+1)^2(\alpha + 1) - \gamma$ implies $\gamma > (k+1)^2$ which is also a contradiction. So if $k^2 < \gamma < (k+1)^2$, $k > 1$, and k is even, one needs $\alpha\gamma < \beta < k^2(\alpha - 1) + \gamma$ and $\beta < (k+1)^2(\alpha + 1) - \gamma$.

(2B) If k is odd

$$F(k\pi) = [k^2(\alpha+1) - \gamma - \beta]\pi^2 \neq 0, \qquad F(\sqrt{\gamma}\pi) = (\alpha\gamma - \beta)\tau^2, \\ F((k+1)\pi) = [(k+1)^2(\alpha-1) + \gamma - \beta)]\pi^2. \tag{A3}$$

If $\alpha\gamma - \beta < 0$ results $F(\sqrt{\gamma}\pi) < 0$ and it should be $F(k\pi) > 0$ and $F((k+1)\pi) > 0$, giving $\beta < k^2(\alpha+1)-\gamma$ and $\beta < (k+1)^2(\alpha-1)+\gamma$. However, $\alpha\gamma < \beta < k^2(\alpha+1)-\gamma$ implies $\gamma < k^2$ (absurd, since $-1 < \alpha$), and $\alpha\gamma < \beta < (k+1)^2(\alpha-1)+\gamma$ implies $\gamma > (k+1)^2$ (absurd, since $\alpha < 1$). On the contrary, if $\alpha\gamma - \beta > 0$ results $F(\sqrt{\gamma}\pi) > 0$ and it should be $F(k\pi) < 0$ and $F((k+1)\pi) < 0$, giving $\beta > k^2(\alpha+1)-\gamma$ and $\beta > (k+1)^2(\alpha-1)+\gamma$. So if $k^2 < \gamma < (k+1)^2$, where $k > 1$ and odd, one needs $k^2(\alpha-1)+\gamma < \beta < \alpha\gamma$ and $(k+1)^2(\alpha+1) - \gamma < \beta$, always under the assumption that $\gamma > 0$ and $|\alpha| < 1$.

In conclusion, the hypotheses of Theorem 2.4 are not only sufficient, but also necessary, in order to have all the roots of P (28) in the left-half plane.

Received xxxx 20xx; revised xxxx 20xx; early access xxxx 20xx.

E-mail address: fsgentile@gmail.com
E-mail address: gitovich@unrn.edu.ar
E-mail address: jmoiola@uns.edu.ar